Dyes and Pigments 196 (2021) 109765

Contents lists available at ScienceDirect

Dyes and Pigments

journal homepage: www.elsevier.com/locate/dyepig

Hymecromone naphthoquinone ethers as probes for hydrogen sulfide detection

Daniel Słowiński [a], Małgorzata Świerczyńska [a], Aleksandra Grzelakowska [a], Marcin Szala [a], Jolanta Kolińska [a], Jarosław Romański [b], Radosław Podsiadły [a,*]

[a] Institute of Polymer and Dye Technology, Faculty of Chemistry, Lodz University of Technology, Stefanowskiego 16, 90-537, Lodz, Poland
[b] Department of Organic and Applied Chemistry, Faculty of Chemistry, University of Lodz, Tamka 12, 91-403, Lodz, Poland

ARTICLE INFO

Keywords:
Dual-mode detections
Coumarin-derived probe
Hydrogen sulfide
Fluorescent probe
Colorimetric probe

ABSTRACT

Hydrogen sulfide (H_2S), as one of the important gasotransmitters, plays an essential role in a many physiological and pathological processes. Commonly used methods for real-time detection and quantification of H_2S are rather complicated. This report presents a simple fluorescence and colorimetry dual-mode assay based on ethers (**Nq-Cm** and **Nq-2Cm**) derived from hymecromone (7-hydroxy-4-methylcoumarin, **Cm**) and naphthoquinone (**Nq**). In these compounds an electron-deficient naphthoquinone unit was used as a suitable reagent for nucleophilic aromatic substitution (S_NAr) reaction. Thiolysis of **Nq-Cm** and **Nq-2Cm** at physiological pH releases **Cm** and causes an significant fluorescence enhancement at 448 nm (with excitation at 320 nm). At the same time, the resulting naphthoquinone derivative **Nq-2SH** causes the solution a purple color, which allows naked-eye detection. Thus **Nq-Cm** and **Nq-2Cm** are colorimetrically selective for H_2S. The efficacy of the **Nq-Cm** and **Nq-2Cm** were demonstrated in buffer with associated submicromolar detection limit as low as 130 nM and 150 nM, respectively. Presented results suggest that both probes are excellent quantitative detection tool for H_2S.

1. Introduction

Cells are the basic fundamentals of life and their metabolism is regulated by many factors, such as gaseous signaling molecules or enzyme levels [1]. Hydrogen sulfide (H_2S) is an endogenous gaseous signaling compound similar to nitric oxide (NO) or carbon monoxide (CO) [2]. Hydrogen sulfide plays an essential role in a many physiological and pathological processes [3–6]. The endogenous hydrogen sulfide is mainly produced by four enzymes: cystathionine beta-synthase (CBS), cystathionine gamma-lyase (CSE), 3-mercaptopyruvate sulfotransferase (MST) and cysteine aminotransferase (CAT) [7,8]. Recently, thiosulfate sulfurtransferase (TST) [9] and selenium-binding protein 1 (SELENBP1) [10] are reported as H_2S producing enzymes. It has been shown that flaws in the enzymes synthesizing H_2S are involved in e.g. cancer [11] and a series of neurodegenerative diseases [4]. It supports tissue growth by stimulating angiogenesis, regulates mitochondrial bioenergetics, stimulates the cell cycle and has anti-apoptotic properties [12,13]. Abnormal level of H_2S is associated with various diseases [14] such as diabetes [15], liver cirrhosis [16], tumors [17], Alzheimer's disease [18] or Down syndrome [19]. Antiviral activity of H_2S has been also demonstrated [20] and in addition, sodium thiosulfate (H_2S-producing compound) has been proposed to treat patients at any stage of the COVID-19 virus infection [21]. Thus, the last decade has brought enormous interest in H_2S releasing agents [22] and its efficient scavengers [23,24]. Hence, it is significant to real time monitor H_2S level to better exploration its biological role and mechanism.

At low levels H_2S was recognized as a tumor growth factor [25,26] whereas the high concentrations of exogenous H_2S could suppress the growth of cancer cells [27]. Thus, H_2S and its donors have been used in antitumor and antimetastatic therapies [28]. Likewise, the ability of H_2S to scavenge the reactive oxygen and nitrogen species depends on kinetic factors i.e., rate constant and concentration of hydrogen sulfide [29].

In this context, not only the detection, but the quantitative determination of H_2S in the *in vitro* and *in vivo* settings is of great importance. Methylene blue (MB) assay, ion selective electrodes (ISE), and gas chromatography [30,31] are quite complex for real-time measurement

* Corresponding author.
E-mail addresses: daniel.slowinski@dokt.p.lodz.pl (D. Słowiński), malgorzata.swierczynska@dokt.p.lodz.pl (M. Świerczyńska), aleksandra.grzelakowska@p.lodz.pl (A. Grzelakowska), marcin.szala@p.lodz.pl (M. Szala), jolanta.kolinska@p.lodz.pl (J. Kolińska), jaroslaw.romanski@chemia.uni.lodz.pl (J. Romański), radoslaw.podsiadly@p.lodz.pl (R. Podsiadły).

https://doi.org/10.1016/j.dyepig.2021.109765
Received 10 May 2021; Received in revised form 30 August 2021; Accepted 30 August 2021
Available online 1 September 2021

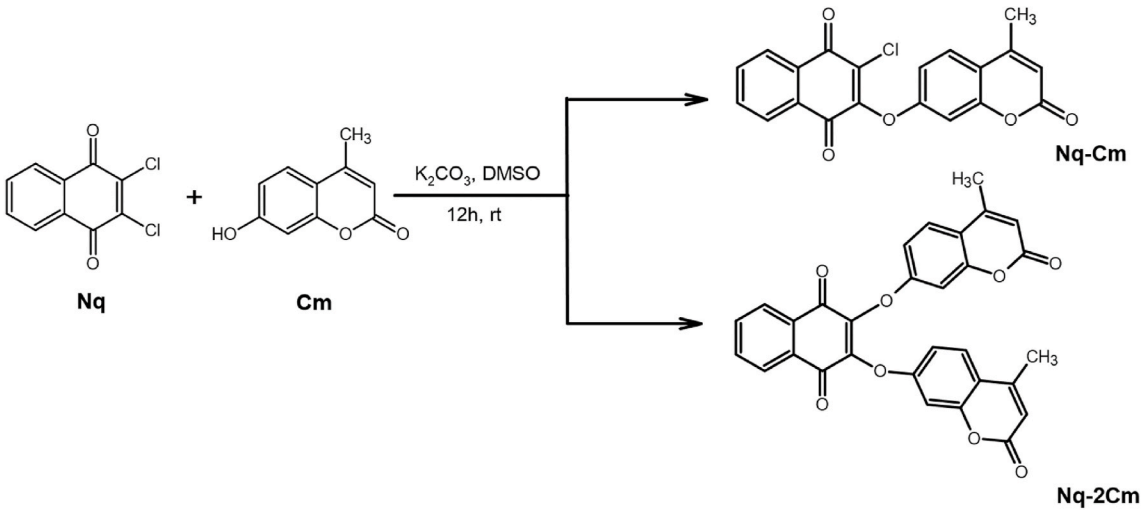

Scheme 1. Synthesis of the **Nq-Cm** and **Nq-2Cm** probes.

of H_2S release. It seems that the best method to quantify of high reactive species including H_2S, could be fluorescence based assays. Fluorescent probes are regarded as a reliable technique due to their high sensitivity, rapid response, real-time detection ability and simple usage [32]. Up to now, several fluorescent probes for H_2S based on azide or nitro group reduction [33–35], copper sulfide precipitation [36,37], nucleophilic addition [38], or thiolysis of ethers [39–41] have been reported. The major drawback of these probes include multi-step synthesis and/or poor stability in water solutions [42]. Conventional probes are prepared by modifying a fluorescent core with a reactive masking moiety which is deprotected by H_2S. This masking group should release the fluorophore only by reaction with hydrogen sulfide [43]. However, only a few of probes can be applied in real biological sample due to slow reaction rate and/or low sensitivity.

In the present work, we used an electron-deficient naphthoquinone [44,45] unit as a suitable reagent for nucleophilic aromatic substitution (S_NAr) reaction, and 4-methyl-7-hydroxycoumarin (**Cm**, hymecromone) as a strong fluorescent dye which serve as a leaving fluorophore. This strategy was inspiration to design and prepare hymecromone naphthoquinone ethers **Nq-Cm** and **Nq-2Cm** as novel probes for H_2S (Scheme 1). Notably, the thiolysis of naphthoquinone ethers has not previously been exploited as mode for fluorescent and colorimetric detection of H_2S. The combination of a fluorescent coumarin and a colored naphthoquinone derivative that are formed in the reaction of the tested ethers with H_2S allows to selectively detect hydrogen sulfide and distinguish it from other biothiols.

2. Experimental

2.1. General

7-Hydroxy-4-methylcoumarin (**Cm**) and 2,3-dichloro-1,4-napthoquinone (**Nq**) were purchased from Merck. Dimethyl sulfoxide (DMSO, reagent grade) used for synthesis was purchased from Chempur. For thin layer chromatography (TLC) pre-coated aluminum-backed plates (Merck Kieselgel 60 F254) was used. Column chromatography purifications were performed on Merck Silica gel 60 (70–230 mesh). ^{1}H NMR and ^{13}C NMR spectra were recorded with a Bruker Avance III 600 using as solvent DMSO-d_6. The high resolution mass spectrum (HRMS) was performed using Synapt G2-Si mass spectrometer equipped with an electrospray ionization (ESI) source and time of flight (TOF) analyzer. The UV–Vis absorption spectra were recorded in a quartz cell of 1 cm path length using the Jasco V-670 UV–vis/NIR spectrophotometer. Fluorescence spectra were measured on spectrofluorometer FLS-920 (Edinburgh Instruments, UK) with both excitation and emission slit widths of 1 nm. The fluorescence quantum yields of **Nq-Cm** and **Nq-2Cm** were determined using 7-hydroxy-4-methylcoumarin ($\Phi = 0.87$ [53]) as reference in PB buffer (0.1 mM, pH 7.4, with 30% MeCN, v/v). The quantum yields were calculated using the following equation (1):

$$\Phi_X = \Phi_{ST}\left(\frac{Grad_x}{Grad_{ST}}\right)\left(\frac{n_x^2}{n_{ST}^2}\right) \quad (1)$$

where, the subscripts *ST* and *X* denote standard and probe respectively, Φ is the fluorescence quantum yield, $Grad_x$ is the slope of the line obtained from the plot of the area of fluorescence vs. absorbance for probe, $Grad_{ST}$ is the slope of the line obtained from the plot of the area of fluorescence vs. absorbance for standard (7-hydroxy-4-methylcoumarin).

2.2. Synthesis of 2-chloro-3-(4-methyl-2-oxo-2H-chromen-7-yloxy) naphthalene-1,4-dione (**Nq-Cm**) and 2,3-bis(2-oxo-2H-chromen-7-yloxy) naphthalene-1,4-dione (**Nq-2Cm**) [47]

To a solution of 7-hydroxy-4-methylcoumarin (0.50 g, 2.9 mmol) in DMSO (20 mL), K_2CO_3 (0.4 g, 2.9 mmol) was added. After 5 min of stirring the 2,3-dichloro-1,4-napthoquinone (0.59 g, 2.6 mmol) was added to the mixture. After stirring at room temperature for 12 h, the resulting mixture was poured into ice water and extracted with EtOAc (2 x 30 mL). Organic layer was washed with 60 mL brine (saturated NaCl solution), dried over Na_2SO_4 and concentrated in vacuo. The mixture of **Nq-Cm** and **Nq-2Cm** was separated by column chromatography (SiO_2) using dichloromethane:methanol (10:1) to obtain pure solid compounds.

Nq-Cm: yellow solid, yield 25%, $R_f = 0.72$, m.p. 214–216 °C

^{1}H NMR (600 MHz) δ (ppm): 8.15 (d, $J = 7.8$ Hz, 1H), 8.02 (d, $J = 8.4$ Hz, 1H), 7.95-7.90 (m, 2H), 7.78 (d, $J = 9.0$ Hz, 1H), 7.41 (d, $J = 2.4$ Hz, 1H), 7.30 (dd, $J_1 = 9.0$ Hz, $J_2 = 2.4$ Hz, 1H), 6.33 (s, 1H), 2.44 (d, $J = 1.2$ Hz, 3H)); ^{13}C NMR (151 MHz): δ (ppm): 178.5; 178.1; 160.2; 159.1; 154.8; 153.6; 152.2; 135.1; 134.9; 132.1; 131.1; 127.5; 127.1; 126.9; 116.0; 113.6; 113.0; 104.2; 18.7. HRMS $[M+H]^+$ for $C_{20}H_{11}ClO_5$ calc. for 367.0378, found 367.0387.

Nq-2Cm: bright orange solid, yield 35%, $R_f = 0.22$, m.p. 219–222 °C

^{1}H NMR (600 MHz) δ (ppm): 8.07-8.04 (m, 2H), 7.95-7.92 (m, 2H), 7.66 (d, $J = 8.4$ Hz, 2H), 7.35 (d, $J = 2.4$ Hz, 2H), 7.22 (dd, $J_1 = 8.7$ Hz, $J_2 = 3.0$ Hz, 2H), 6.27 (d, $J = 1$ Hz, 2H), 2.39 (s, 6H). ^{13}C NMR (151 MHz): δ (ppm): 180.2; 160.2; 159.5; 154.6; 153.5; 146.0; 134.9; 131.6; 127.1; 126.5; 115.8; 113.7; 112.9; 104.5; 18.6. HRMS $[M+H]^+$ for $C_{30}H_{18}O_8$ calc. for 507.1085, found 507.1080.

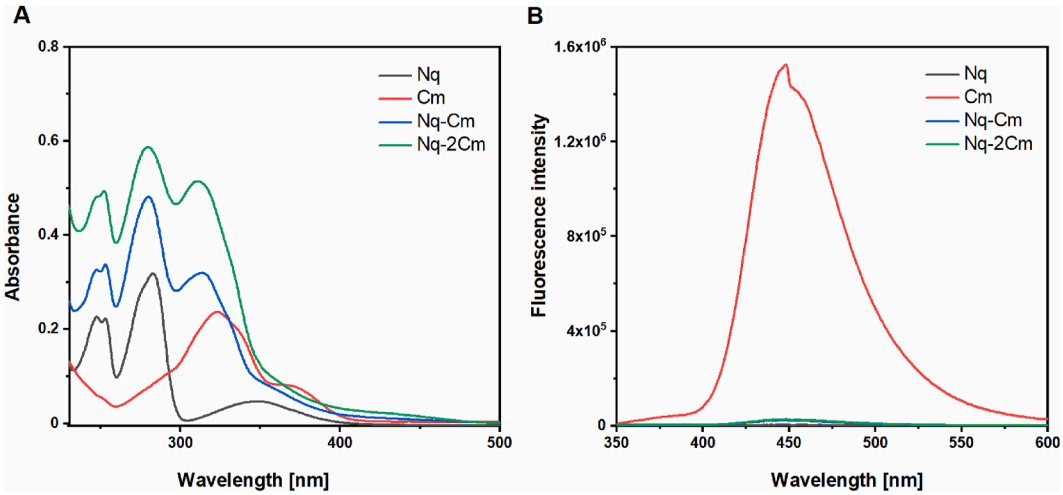

Fig. 1. (A) UV–Vis absorption and **(B)** emission spectra of **Nq**, **Cm**, **Nq-Cm** and **Nq-2Cm** recorded in a phosphate buffer (0.1 M, pH 7.4) containing acetonitrile (30%). λ_{ex} = 320 nm, slites 1.0/1.0 nm.

2.3. UV–vis and fluorescence measurements

All spectroscopic measurements were performed in a phosphate buffer (0.1 M, pH 7.4) containing acetonitrile (MeCN), (30%, v/v) at room temperature. Phosphate buffer solution (0.1 M) was made by mixing 0.2 M solution of $Na_2HPO_4 \times 12H_2O$, 0.2 M solution of $NaH_2PO_4 \times 2H_2O$ and water. Compounds were dissolved in MeCN to prepare 1 mM stock solution. Before measurements probe stock solution was diluted with buffer (0.1 M, pH 7.4) containing MeCN (30%) to afford the final concentration of 2–80 μM. Stock solution of Na_2S (1 mM) in phosphate buffer (PB) was used as H_2S source. To evaluate of H_2S concentration in phosphate buffer, we used Ellman's reagent, i.e., 5,5′-dithiobis(2-nitrobenzoic acid) (DTNB). Detail procedure is described in Supporting Information. Various sodium salt stock solutions (1 mM; Cl^-, Br^-, I^-, CO_3^{2-}, SO_4^{2-}, $S_2O_4^{2-}$, SO_3^{2-}, HSO_3^-) were freshly prepared by dissolving weighed portions of the corresponding salts in deionized water. Stock solution of biothiols (1 mM): L-cysteine (L-Cys), L-glutathione (L-GSH), *N*-acetyl-L-cysteine (NAC) were also prepared in deionized water. Stock solution (1 mM) of chemical reducing agent: sodium borohydride ($NaBH_4$) and biological reductant NADPH were freshly prepared in methanol and deionized water, respectively. The reduction of probes using sodium borohydride was performed in an organic solvent (MeCN). After 30 min of reaction, phosphate buffer was added and the emission spectra were measured. All measurements were performed in a 3.5 mL quartz cuvette with 3 mL solution. The reaction mixture was shaken uniformly at room temperature before measurements. For fluorescence measurement excitation wavelength was set at 320 nm.

The limit of the detection was calculated from equation (2):

$$LOD = 3.3\sigma/S \quad (2)$$

where, σ is the standard deviation of probe solution (blank), S is the slope of the linear calibration plot between the fluorescence emission intensity and the concentration of Na_2S.

2.4. HPLC measurements

HPLC analyses of **Cm**, **Nq-Cm** and **Nq-2Cm** were performed using UFLC Shimadzu equipped with UV–Vis absorption and fluorescence detector. Analyses were done using a Kinetex C_{18} column (Phenomenex 100 mm x 46 mm, 2.6 μm) which was equilibrated with 10% of MeCN in water, containing 0.1% trifluoroacetic acid (TFA). The standards and products formed in the reaction of **Nq-Cm** or **Nq-2Cm** with H_2S were eluted by an increase of MeCN concentration from 10 to 100% over 12 min at the flow rate of 1.5 mL/min. The HPLC traces of **Nq-Cm, Nq-2Cm** and coumarin (**Cm**) formed in reaction with H_2S were detected by monitoring the absorption at 330 nm.

3. Results and discussion

3.1. Synthesis and optical characterizations

Coumarins have good stability and desired spectroscopic properties i.e. excitation and emission in UV region, large molar extinction coefficient and good fluorescence quantum yield [46]. Hydroxyl group at position C-7 in the coumarin allows for relatively easy addition of fluorescence quenching trigger. **Nq-Cm** and **Nq-2Cm** were synthesized from commercially available reagents by coupling of 7-hydroxy-4-methylcoumarin (**Cm**) with 2,3-dichloro-1,4-naphthoquinone (**Nq**) at room temperature (Scheme 1) according to slightly modified procedure [47]. Identity of **Nq-Cm** and **Nq-2Cm** was confirmed by means of ^1H

Table 1
Spectroscopic properties of **Nq**, **Cm**, **Nq-Cm** and **Nq-2Cm** in acetonitrile.

Compound	λ_{max} (nm)	ε (λ_{max}) ($M^{-1}\cdot cm^{-1}$)	λ_{exc} (nm)	λ_{em} (nm)	Φ_{em}[e] (%)	Stokes shift (nm)	pKa	E
Nq	272[a]	16500	n/a	n/a	n/a	n/a	n/a	−0.45
Cm	323[b]	12420	320	450	87 [53]	127	7.8[c]	0.7[d]
Nq-Cm	279,313	24150,16000	320	448	7.7	135	n/a	n/a
Nq-2Cm	279,313	29700, 26000	320	448	7.8	135	n/a	n/a

[a] in a 0.1 M Tris buffer (pH 8.5) from Ref. [51].
[b] in PBS from Ref. [52].
[c] in PB buffer from Ref. [49].
[d] in PBS buffer from Ref. [50].
[e] using 7-hydroxy-4-methylcoumarin (**Cm**) (Φ = 0.87) as reference [53].

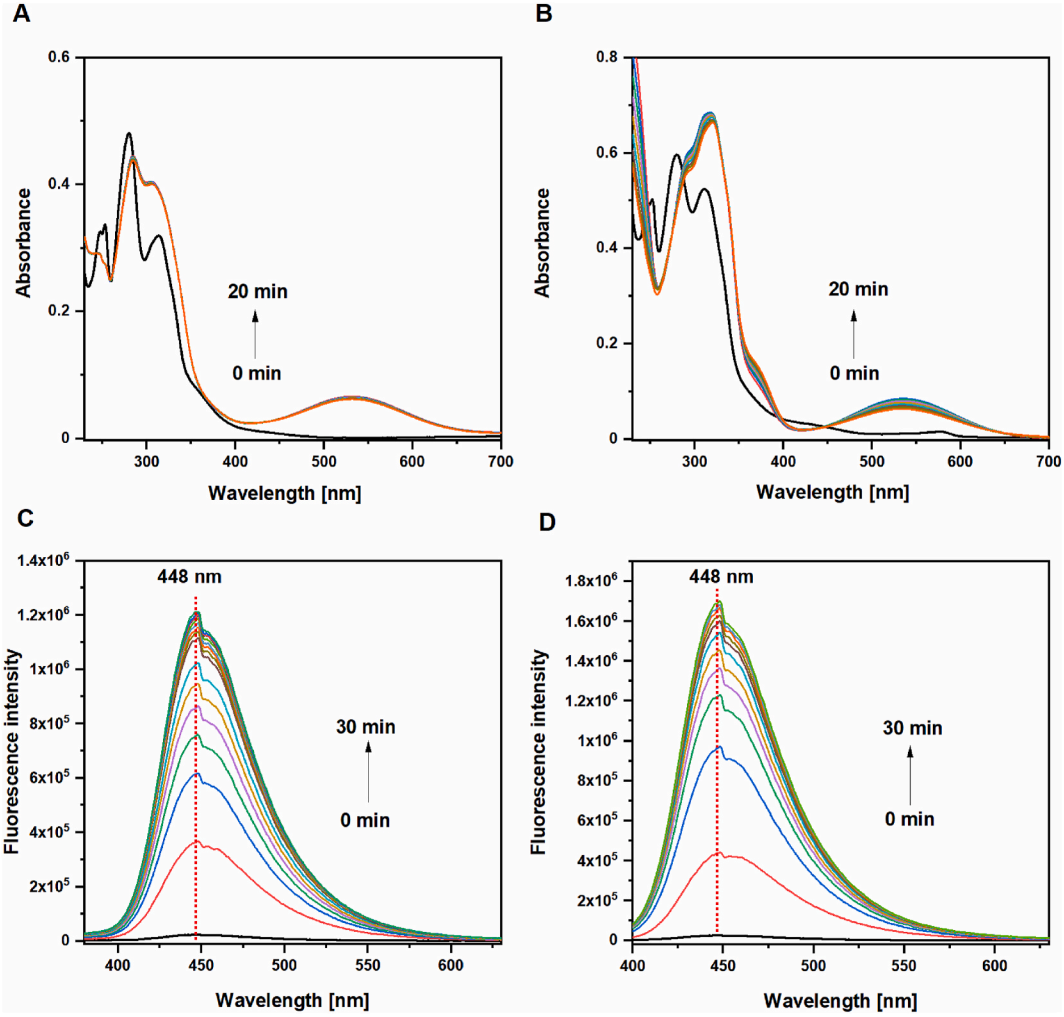

Fig. 2. (A), (B) Time-depended absorbance spectra of **Nq-Cm** and **Nq-2Cm** (20 μM) recorded after bolus addition of Na_2S (80 μM). **(C), (D)** Time depended fluorescence spectra (λ_{ex} = 320 nm) of **Nq-Cm** and **Nq-2Cm** (5 μM) after bolus addition of Na_2S (20 μM).

NMR, ^{13}C NMR and HRMS spectroscopy (see Supplementary Information (SI), Figures S12-S19).

First, we tested the solubility of **Nq-Cm** and **Nq-2Cm** in PB buffer solutions containing MeCN (30%, v/v). The linear dependence of the absorbance on the concentration of the probes in the range at 2–20 μM (Fig. S1) confirms the possibility of performing all tests in such solution. Next, we compared the spectroscopic properties of **Nq-Cm** and **Nq-2Cm** with the 7-hydroxy-4-methylcoumarin (**Cm**) and 2,3-dichloro-1,4-naphthoquinone (**Nq**). The absorbance and emission profiles are illustrated in Fig. 1. As shown in Fig. 1A, studied ethers have absorption bands located approx. at 279 nm and 313 nm, which can be assigned to the **Nq** and **Cm** core, respectively. Small negative reduction potentials [48] make **Nq** act as good electron acceptor. The influence of **Nq** on photophysical properties of **Nq-Cm** and **Nq-2Cm** is clearly visible when we compare the fluorescence quantum yield of **Cm** and its ethers. The data presented in Table 1 clearly shows that **Nq-Cm** and **Nq-2Cm** have

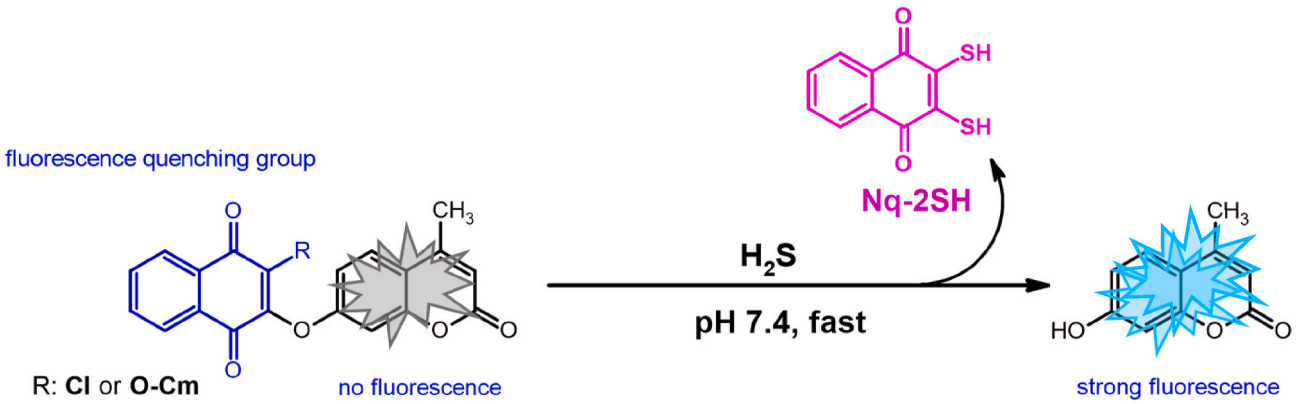

Scheme 2. The sensing mechanism of probes for H_2S.

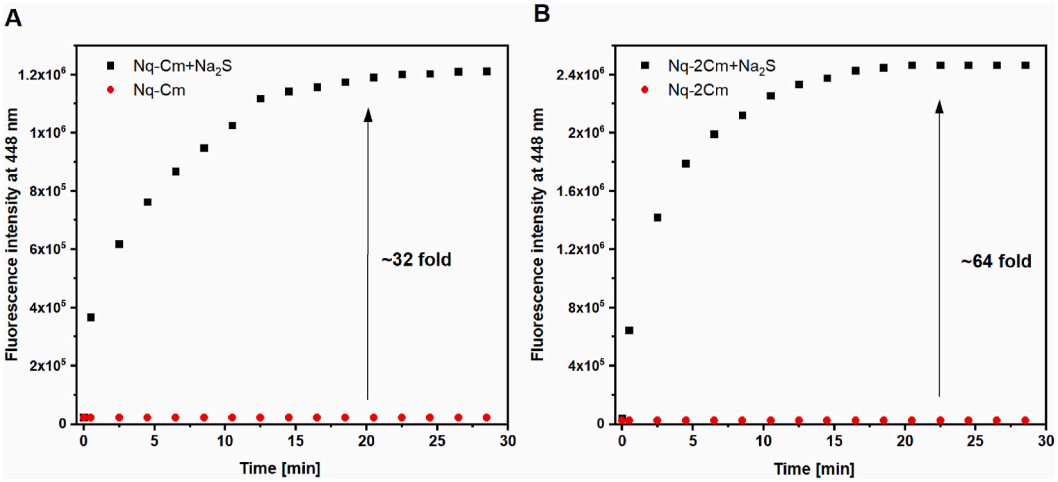

Fig. 3. Reaction time profiles of **Nq-Cm** and **Nq-2Cm** (5 μM) alone or in the presence of H_2S (20 μM) in PB buffer (0.1 M, pH 7.4 containing 30% MeCN v/v), λ_{ex} = 320 nm, slites 1.0/1.0 nm.

an emission band located at the same wavelength as **Cm**. Only the fluorescence quantum yield of ethers is ten times lower compared to the quantum yield of the parent coumarin. Both probes exhibit a weak fluorescence ($\Phi < 0.08$) in PB buffer (0.1 M, pH 7.4, with 30% MeCN, v/v). Thus, the release of the **Cm** fluorophore from **Nq-Cm** and **Nq-2Cm** will result in the activation of fluorescence.

*3.2. UV–vis and fluorescence response of **Nq-Cm** and **Nq-2Cm** toward H_2S*

To investigate our hypothesis that naphthoquinone-derived probes are a suitable platform for creating H_2S sensitive "turn-on" sensors, we study the reactivity of **Nq-Cm** and **Nq-2Cm** in the presence of H_2S. Initially, we checked if the addition of Na_2S (as an aqueous source of hydrogen sulfide) will cause the release of **Cm** from **Nq-Cm** and **Nq-2Cm**. Fig. 2 shows the changes in the absorption and emission spectra of the probes recorded within 20 min after mixing of tested ethers with Na_2S. After addition of the analyte to the solution of **Nq-Cm** or **Nq-2Cm** we observed three alterations: (i) increase of the absorption band at 325 nm, (ii) emergence a new wide band at around 530 nm and (iii) decrease of the absorption band at 279 nm. Both probes reacting with the hydrogen sulfide source give a very fast fluorescent response. After the first minutes of the reaction, the fluorescence intensity increases several times and may be sufficient to confirm the presence of hydrogen sulfide or its donors in various biosystems. The resulting fluorescent spectra of **Nq-Cm** and **Nq-2Cm** after addition of Na_2S show a maximum fluorescence intensity at the same wavelength as 7-hydroxy-4-methylcoumarin. Those results suggest that H_2S had cleaved the ether bond in **Nq-Cm** and **Nq-2Cm**, releasing the fluorescent coumarin (Scheme 2). 2,4-Naphtoquinone unit effectively quenches the emission of fluorophore *via* the photoinduced electron transfer (PET) effect. After treatment with H_2S, the electron-donating ability of the hydroxyl group of **Cm** came into play and triggered the ICT process, and the fluorophore induces a strong blue fluorescent signal. Moreover, the intensity of the absorption bands located at 319 nm and 530 nm increase, which could be assign to the formation of **Cm** and **Nq-2SH**, respectively. Additionally, we confirmed that gaseous hydrogen sulfide converted the probes (see SI, Figures S7 and S8) in the same way as Na_2S.

To confirm the proposed sensing mechanism the reaction mixtures were analyzed by high resolution mass spectrometry (HRMS). HRMS spectra confirmed in both cases formation of 7-hydroxy-4-methylcoumarin (**Cm**). A peak located at 175.04 corresponding to **Cm** ($C_{10}H_8O_3$, $[M - H]^-$:175.16) was observed. In addition analysis confirmed the formation of **Nq-2SH** (peak at 220.97; $C_{10}H_6O_2S_2$) as a second product of thiolysis of both probes (see SI, Figures S17 and S19). The analysis also showed the formation of the **Nq-SH-Cm** intermediate with one –SH

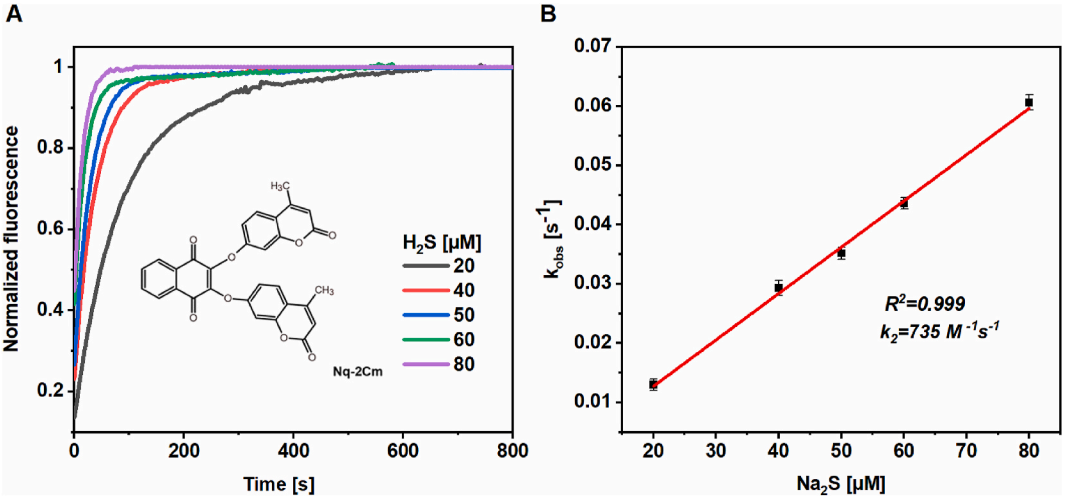

Fig. 4. (A) The time-dependent fluorescence intensity at 448 nm for **Nq-2Cm** (2 μM) in the presence of different concentrations of Na_2S in PB buffer (0.1 M, pH 7.4, containing 30% MeCN, v:v), **(B)** The linear relationship of k_{obs} versus Na_2S concentrations.

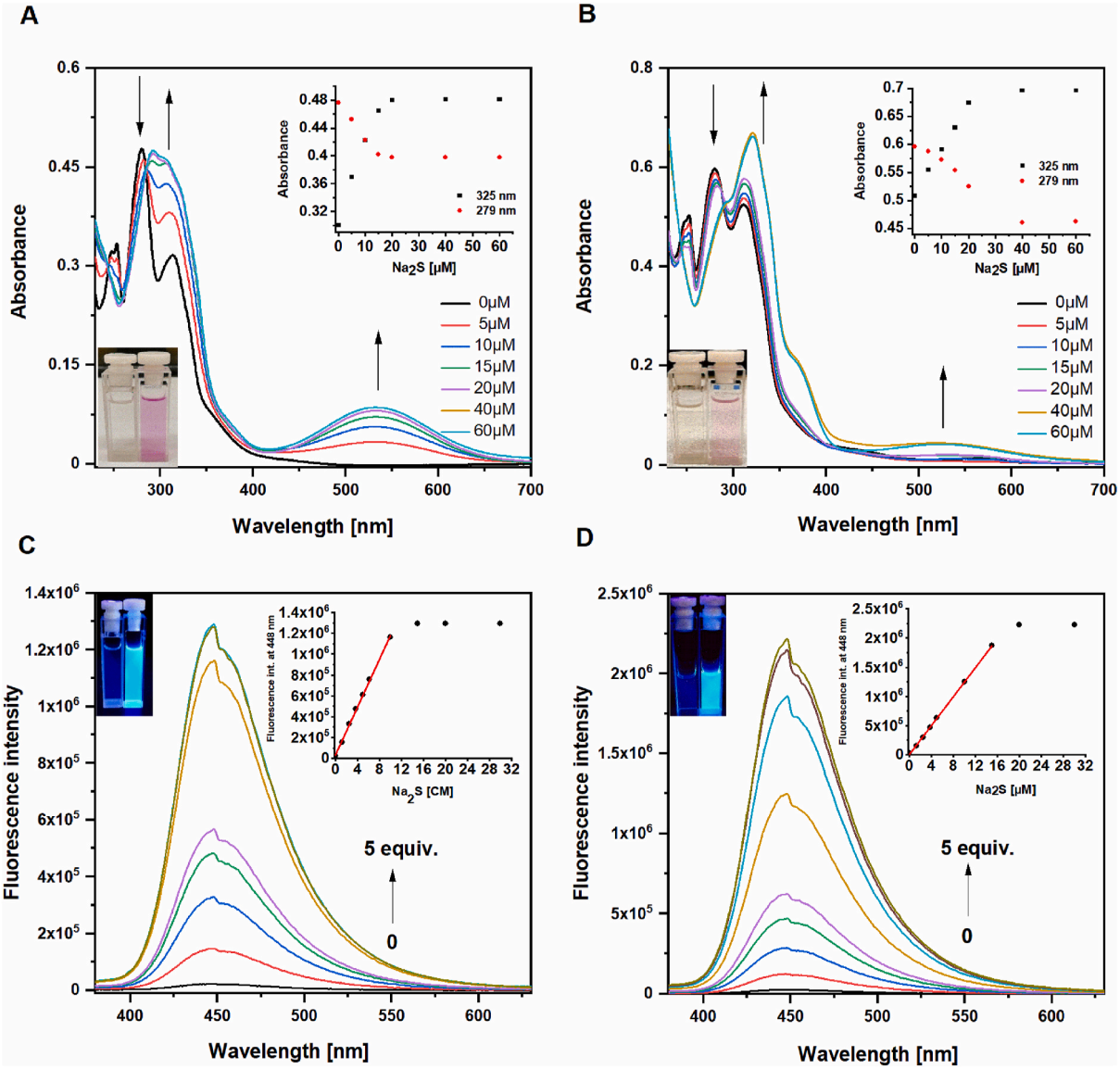

Fig. 5. (A), (B) Absorption spectral change of **Nq-Cm** and **Nq-2Cm** (20 μM) response to various concentration of Na_2S (0–60 μM) in PB buffer (0.1 M, pH 7,4, containing 30% MeCN, v/v) after 15 min of incubation; Photos of the quartz cuvettes before and after the addition of Na_2S **(C), (D)** The fluorescence change of **Nq-Cm** and **Nq-2Cm** (5 μM) response to various concentration of Na_2S (0–25 μM) in PB buffer (0.1 M, pH 7,4, containing 30% MeCN) after 15 min of incubation, excitation is 320 nm, slites 1.0/1.0 nm, Inset: **5 (A), (B)** The plot of absorbance changes at 325 and 279 nm upon addition of Na_2S; **(C), (D),** fluorescence intensity changes at 448 nm of **Nq-Cm** and **Nq-2Cm** as a function of Na_2S concentrations. Photos of the quartz cuvettes before and after the addition of Na_2S under UV light.

group (peak at 363.03, $C_{20}H_{12}O_5S$).

Recorded fluorescence and absorption spectra allow to determine the time needed to release the maximum amounts of **Cm** and **Nq-2SH** from the studied probes. Fig. 2 reveals that the maximum fluorescence response of both tested probes occurs in approximately 15 min after the addition of sodium sulfide. Additionally, after this time, we did not observe any changes in the absorption spectra.

The recorded time-dependent fluorescence (Fig. 3) showed that the maximal fluorescence signals were reached within 15 min with a 32 fold and 64 fold enhancement for **Nq-Cm** and **Nq-2Cm**, respectively. In the absence of any analyte, no significant change of fluorescence intensity of **Nq-Cm** or **Nq-2Cm** was observed, indicating that both probes possess a good stability in the system. Our results indicate that sensors may be useful for detection of H_2S.

We also tried to determine the pseudo-first-order rate constant by measuring fluorescent response of **Nq-Cm** after addition of Na_2S in phosphate buffer (pH 7.4) at 25 °C. However, the reaction is too fast to be measured with the aid of steady-state fluorescence spectra. Reaction kinetics, as an important parameter, was only investigated for the **Nq-2Cm** probe due to its slower reaction with Na_2S. The time-dependent fluorescence at 448 nm was recorded for data analysis (Fig. 4A). The pseudo-first order rate (k_{obs}), was found by fitting the data with a single exponential function (Fig. S4). The reaction rate k_2 ($7.35 \times 10^2\ M^{-1}s^{-1}$) was obtained by linear fitting of the k_{obs} versus Na_2S concentration (Fig. 4B). The reaction rate between probe and Na_2S is much faster than the reaction rate of most fluorescent or colorimetric probes based on various fluorophores [54,55], implying that **Nq-2Cm** can scavenge H_2S efficiently. Because there are at least two steps in **Cm** release from the probe, the rate constant should be treated as an apparent rate constant, which is influenced by the kinetics of at least two steps of the reaction.

3.3. *Absorption and fluorescence titration*

In the next step, we measured the changes of ethers response towards increasing Na_2S concentration. The absorption spectra were recorded after 15 min of incubation. As depicted in Fig. 5A and B, with increasing

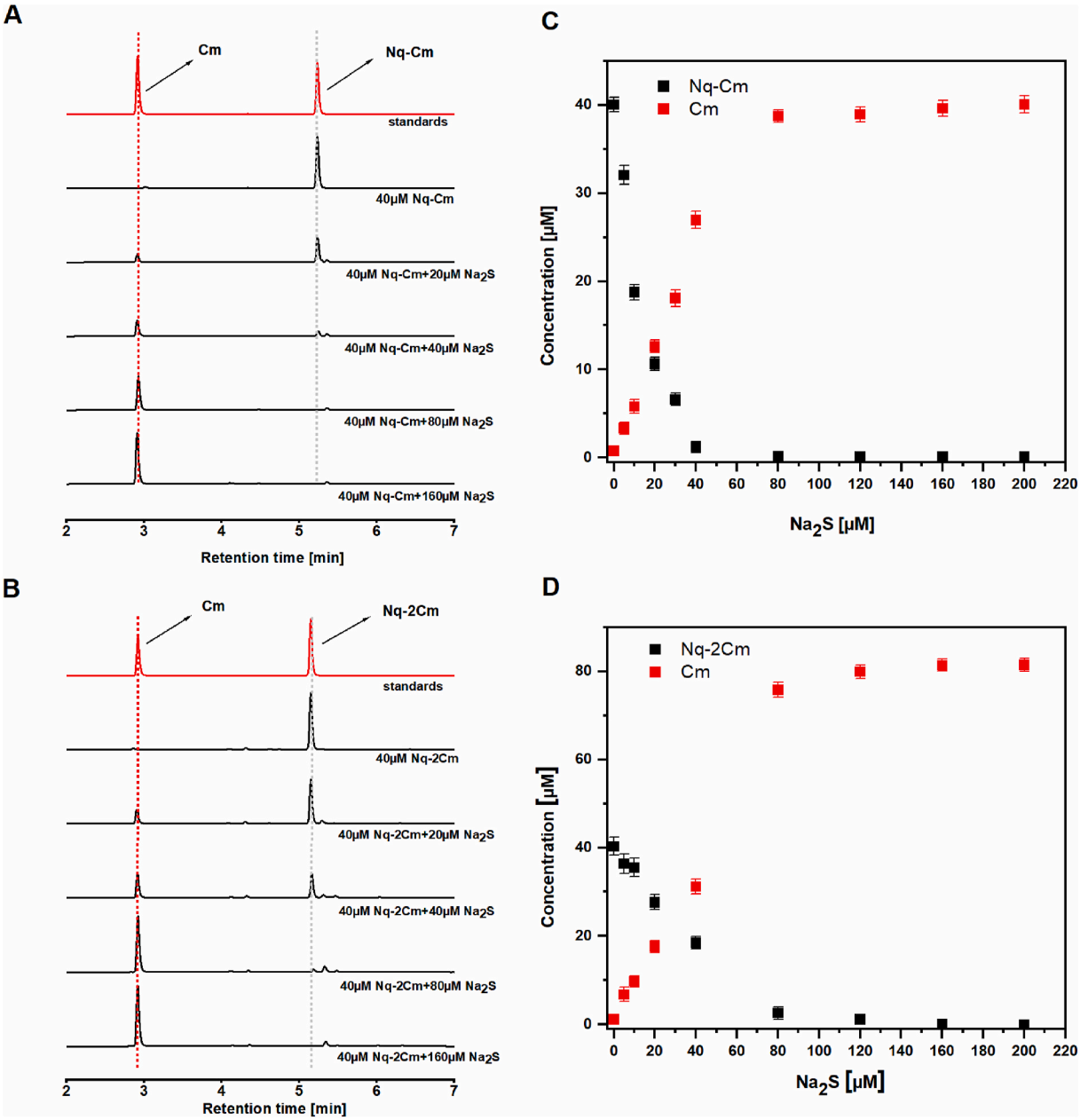

Fig. 6. HPLC chromatogram of the standards (40 μM) and reaction mixtures of **(A) Nq-Cm** (40 μM) and **(B) Nq-2Cm** with Na_2S (0–160 μM) after 15 min of incubation. The traces were collected using an absorption detector set at 330 nm. HPLC-based titration of **(C) Nq-Cm** (40 μM) and **(D) Nq-2Cm** (40 μM) with Na_2S after 15 min of incubation in solution. Data are means ± standard deviation of three independent experiments.

Na_2S concentration, the absorption band at 279 nm slowly decreases and simultaneously the absorption band at 325 nm increases, along with an appearance of new absorption band at 530 nm. The same absorption band was formed when we mixed **Nq** with Na_2S (see SI, Fig. S9), whereas an bolus addition of Na_2S into the solution of **Cm** did not change its absorption and fluorescence spectra (see SI, Fig. S11). The two-fold and greater excess of sodium sulfide used during titration do not affect the absorption spectrum of the **Nq-Cm** and **Nq-2Cm** ethers. Fig. 5C and D show that intensity of fluorescence emission of probes at 448 nm also increase when Na_2S was added gradually (0–5 equiv.) into the solution. In addition, the fluorescence intensity was linearly connected with concentrations of Na_2S ranging from 0 to 10 μM for **Nq-Cm** and from 0 to 15 μM for **Nq-2Cm** (insets in Fig. 5C and D). The limit of detection (LOD) based on fluorescent measurements was calculated to be 130 nM for **Nq-Cm** and 150 nM for **Nq-2Cm**. These results suggest that the probes are a good quantitative detection tools for H_2S. Additionally, the fluorescence intensity after reaction of **Nq-2Cm** with H_2S is twice as high as the fluorescence intensity during **Nq-Cm** titration with H_2S. This may suggests that two coumarin molecules are released during the reaction of the **Nq-2Cm** probe with the analyte (H_2S).

3.4. HPLC titrations

Our spectroscopic investigations showed that the mixing of the probes with Na_2S turns on a blue fluorescence and a purple color of the solution. Therefore, we conducted HPLC analyses to detect the formed products and to determine the stoichiometry of the reaction between probes and Na_2S. HPLC chromatograms and stoichiometric analyses are shown in Fig. 6. These chromatograms show the slow disappearance of naphthoquinone ethers (**Nq-Cm** and **Nq-2Cm**) and the formation of a fluorescence product with the retention time of 2.9 min. Comparison of the retention time of the authentic standard of 7-hydroxy-4-

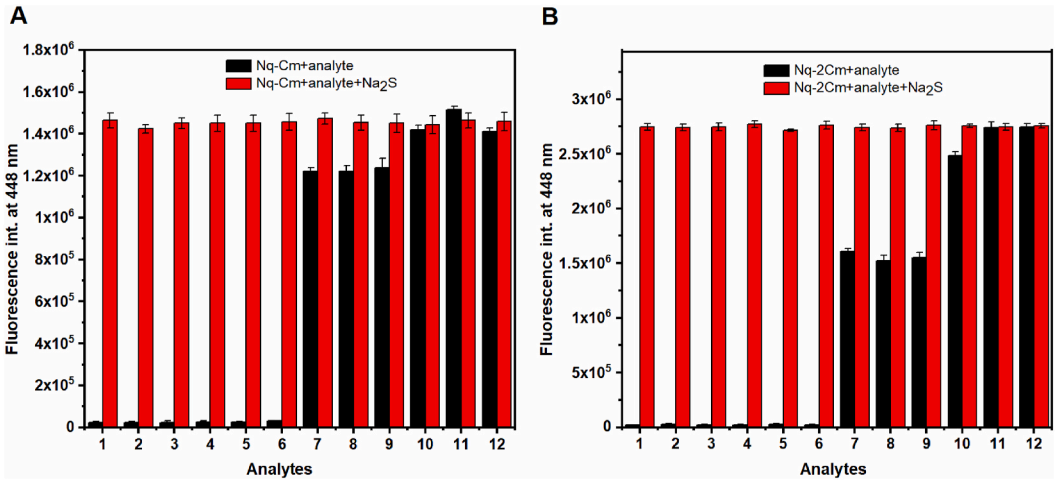

Fig. 7. The fluorescence intensity changes of probe **Nq-Cm** (5 μM) **(A)** and **Nq-2Cm** (5 μM) **(B)** upon addition of various species (25 μM for each). 1. Blank; 2. Cl^-; 3. Br^-; 4. I^-; 5. CO_3^{2-}; 6. SO_4^{2-}, 7. SO_3^{2-}; 8. HSO_3^-; 9. $S_2O_4^{2-}$; 10. L-Cys; 11. L-GSH; 12. NAC. Data are means ± standard deviation of three independent experiments.

methylcoumarin (**Cm**) confirms that **Cm** is one of the products found in the reaction mixture. Additionally, HPLC analysis showed that **Cm** is not a sole product of the Na_2S-induced **Nq-Cm** or **Nq-2Cm** conversion. The new compound with the retention time of 5.34 min was formed. To monitor a Nq-derivative product we also recorded a HPLC trace at 530 nm (Fig. S3). At this wavelength, for both probes only one product (with a retention time of 5.34 min) was detected, which indicates the formation of **Nq-2SH** as probes thiolysis product. Stoichiometric analysis

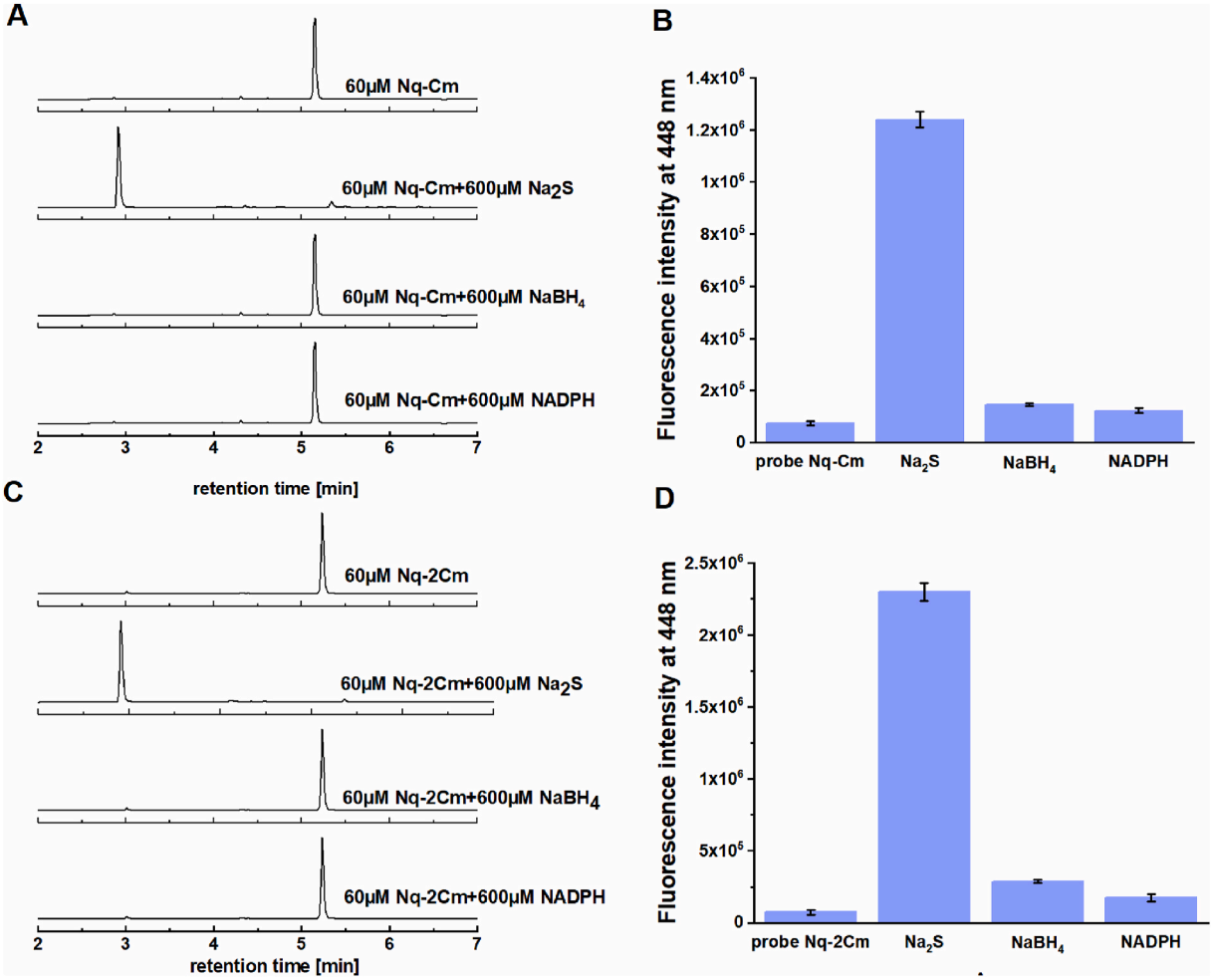

Fig. 8. (A), (C) HPLC chromatogram of **Nq-Cm**, **Nq-2Cm** (each 60 μM) and the reaction mixture of probes with Na_2S, $NaBH_4$, NADPH (each 600 μM). Incubation time was 30 min. The traces were collected using an absorption detector set at 330 nm, **(B), (D)** Emission of **Nq-Cm** and **Nq-2Cm** (each 5 μM) before and after addition of Na_2S, $NaBH_4$, NADPH (each 50 μM) after 30 min of incubation in PB buffer (0.1 M, pH 7.4, containing 30% MeCN, v. v). Data are means ± standard deviation of three independent experiments.

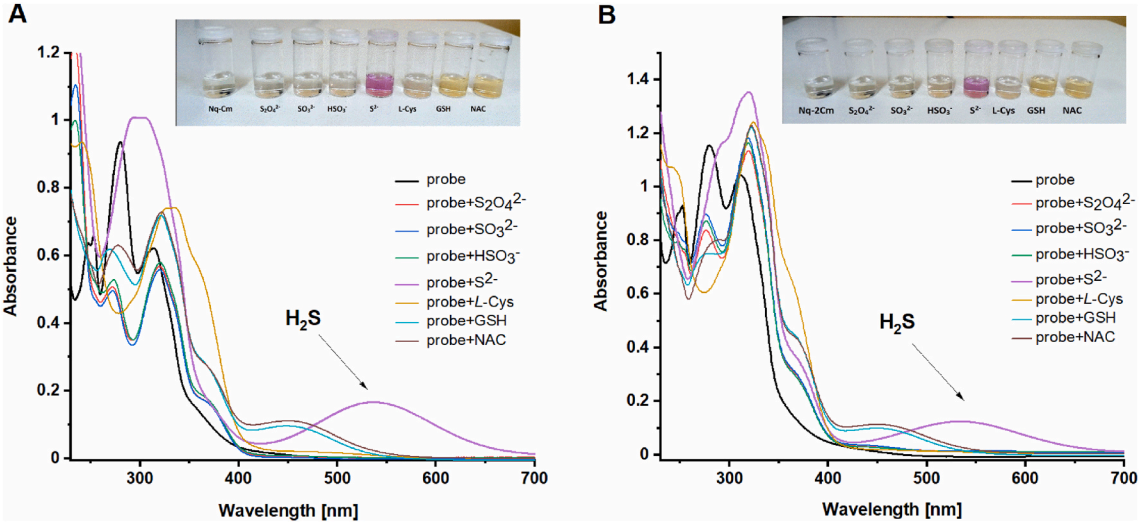

Fig. 9. Absorption spectral changes of **Nq-Cm** and **Nq-2Cm** (each 40 μM) response to various sulfur species (200 μM) after 15 min of incubation.

shows that both probes are completely consumed by Na_2S. However, the amount of **Cm** released depends on the chemical structure of the probe. Mono- and bis-hymecromone naphthoquinone ethers (**Nq-Cm** and **Nq-2Cm**) produce one and two equivalents of **Cm**, respectively (Fig. 6C and D). Moreover, the **Nq-Cm** probe due to the reactivity of the chlorine atom in the naphthoquinone ring, firstly form the **Nq-SH-Cm** intermediate followed by released of **Cm** in the reaction of **Nq-SH-Cm** with Na_2S. As a result, the release of coumarin from **Nq-Cm** requires two equivalents of Na_2S. As the **Nq-SH-Cm** intermediate is nonfluorescent, colored compound, the differences in the stoichiometry of the changes in absorbance (1:1) and fluorescence (1:2) of **Nq-Cm** in response to Na_2S were also observed (Fig. 5A and C).

3.5. Selectivity of and co-interference studies

Promising, described above results, allows to expand investigation for the selectivity and sensitivity of the **Nq-Cm** and **Nq-2Cm** probes. To study of selectivity the various analytes, including Na_2S, selected anions, sulfur species and biothiols, were added to the probes solution and the fluorescence responses were recorded. As shown in Fig. 7, Na_2S as expected induced obvious fluorescence enhancement. We also observed a significant fluorescent signal growth in the case of biothiols: L-glutathione (L-GSH), L-cysteine (L-Cys) and *N*-acetyl-L-cysteine (NAC). This result is not entirely satisfactory, however the good probe should has a high selectivity and does not react with other compounds. On the other hand, this result was expected, because L-Cys, L-GSH and NAC along with H_2S, belong to biothiols and have similar properties. Therefore, it is difficult to design a selective probe for H_2S and biothiols. Fluorescence measurements with the aid of **Nq-Cm** and **Nq-2Cm** will report total biothiols, however the usage of colorimetry and/or HPLC-based monitoring of the Nq-derived product will help identify the analyte. It is also worth mentioning that hydrogen sulfide, due to its lower pKa than L-cysteine, reacts faster with the probe, which causes a rapid fluorescence response. It may seem that probes for H_2S based on the azide reduction mechanism are less sensitive to other sulfur-containing compounds. The reactive systems used do not change the fluorescence intensity after the addition of e.g. L-Cys or H_2S [56].

We also examined how the probes behaved in the presence of a chemical reductant ($NaBH_4$) and a biological reducing agent (NADPH). It is well known that strong reductants can reduce carbonyl-containing compounds such as ketones or aldehydes and quinones to alcohols and hydroquinones [57]. Due to the potential usage of probes in biological systems, it was necessary to test the stability of the probes in the presence of these reducing agents. Using HPLC and spectrofluorimetry we

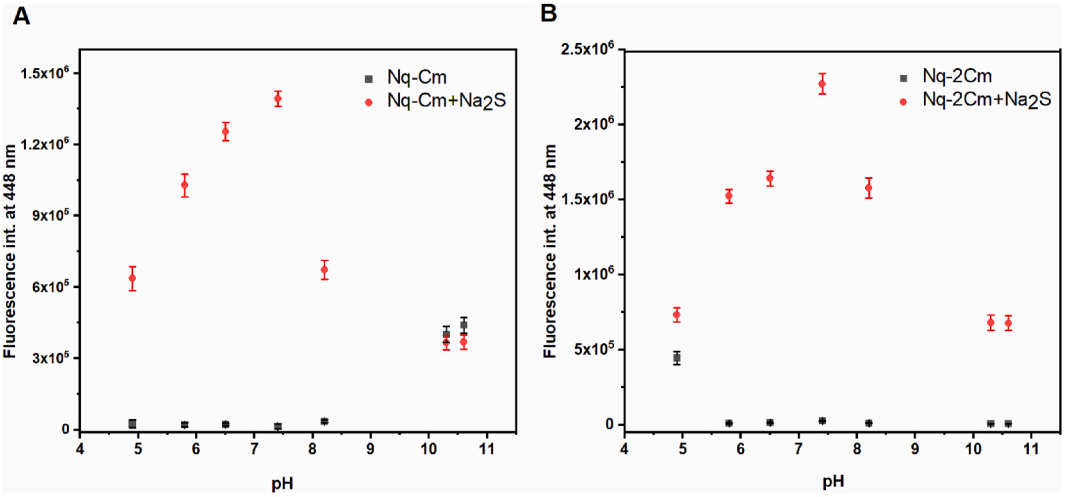

Fig. 10. The fluorescence intensity of **Nq-Cm** and **Nq-2Cm** (each 5 μM) in the absence and presence of Na_2S (25 μM) in different pH buffer solutions (λ_{ex} = 320 nm, slites 1.0/1.0 nm). Data are means ± standard deviation of three independent experiments.

tested the stability of **Nq-Cm** and **Nq-2Cm** in solution with reducing agents (Fig. 8). The addition of a 10-fold excess of reductants did not affect the stability of the probes. HPLC chromatograms show the absence of new product(s) formation, and the recorded fluorescence intensities were independent of the reductants addition and were not changed during a prolonged incubation time. Thus, $NaBH_4$ or NADPH had no effect on the probes.

Additionally, we investigated the absorption changes of probes toward important biothiols and sulfur species. Both probes mixed only with Na_2S give a new absorption band at 530 nm, that results as the violet color of the solution (Fig. 9). This is a satisfactory result because the **Nq-Cm** and **Nq-2Cm** are colorimetrically selective for biothiols and sulfur-containing anions. However, only for Na_2S appearance of new absorption bands at 530 nm was observed, which distinguishes H_2S from L-glutathione, L-cysteine and *N*-acetyl-L-cysteine. Utilization of fluorescence and colorimetric techniques for these probes confirm the presence of hydrogen sulfur in the tested system.

3.6. *Influence of pH on the fluorescence response of **Nq-Cm** and **Nq-2Cm***

To determine the usefulness of **Nq-Cm** and **Nq-2Cm** under physiological conditions, their responses toward H_2S under various values of pH have been studied. The change of fluorescence intensity of probes induced by H_2S was investigated in the pH range of 4–11. Fig. 10 shows the relation of fluorescence of **Nq-Cm** or **Nq-2Cm** in the absence (in black) and presence (in red) of Na_2S. As can be seen, probes are very stable over the pH range of 5–10 and the strong fluorescent in the pH range of 7–8 is visible only in the presence of Na_2S. In the pH $>$ 7.5 fluorescent intensity was decreased with increasing pH level. Similar results have been also obtained by other researchers working with fluorescent probes based on hydroxycoumarins for detection of various biothiols [58,59]. Since both acetonitrile (Fig. S2) and Na_2S (Fig. S11) do not significantly affect the fluorescence intensity, the observed effect may be related with the interaction of **Nq-SH-Cm** or **Nq-2SH** with the coumarin anion.

4. Conclusions

In summary, **Nq-Cm** and **Nq-2Cm** probes derived form 7-hydroxy-4-methylcoumarin (**Cm**) and 2,3-dichloro-1,4-napthoquinone (**Nq**) have been synthesized. These probes show rapid and significant fluorescence response in the blue emission region when Na_2S, as hydrogen sulfide donor, is added to the phosphate buffer. Although L-Cys, L-GSH, and NAC also induce fluorescence, the combine usage of colorimetry and/or HPLC-based monitoring of the Nq-derived product can identify H_2S (Na_2S). The convenient detection process (within 15 min), a good linearity range, and a low detection limit of H_2S (130 nM, 150 nM) give a great advantages of **Nq-Cm** and **Nq-2Cm**. All of these relevant results suggest that these probes can be applied as a valuable tools for detection of H_2S in living systems.

Author contributions

Daniel Słowiński: Investigation, Methodology, Formal analysis; Writing. Małgorzata Świerczyńska: Investigation. Aleksandra Grzelakowska: Methodology, Investigation. Marcin Szala: Methodology, Investigation. Jolanta Kolińska: Methodology, Investigation Jarosław Romański: Writing – review & editing. Radosław Podsiadły: Conceptualization, Investigation, Methodology, Resources, Writing – review & editing, Supervision. All authors reviewed the results and approved the final version of the manuscript.

Declaration of competing interest

The authors declare that they have no known competing financial interests or personal relationships that could have appeared to influence the work reported in this paper.

Acknowledgements

This work was supported by the National Center for Research and Development (Warsaw, Poland) within the grant InterChemMed (POWR.03.02.00–00-I029/16)

Appendix A. Supplementary data

Supplementary data to this article can be found online at https://doi.org/10.1016/j.dyepig.2021.109765.

References

[1] Fu M, Zhang W, Wu L, Yang G, Li H, Wang R. Hydrogen sulfide (H_2S) metabolism in mitochondria and its regulatory role in energy production. Proc Natl Acad Sci USA 2012;109(8):2943–8. https://doi.org/10.1073/pnas.1115634109.
[2] Jiang N, Wang B, Liu T, Liu Q, Wei Q, Xing Y, Zheng G. Fast and sensitive fluorescent probe for ratiometric detection of hydrogen sulfide in mitochondria. Anal. Methods 2019;11:232–5. https://doi.org/10.1039/c8ay02586j.
[3] Wang R. Physiological implications of hydrogen sulfide: a whiff exploration that blossomed. Physiol Rev 2012;92:791–896. https://doi.org/10.1152/physrev.00017.2011.
[4] Wallace JL, Wang R. Hydrogen sulfide-based therapeutics: exploiting a unique but ubiquitous gasotransmitter. Nat Rev Drug Discov 2015;14:329–45. https://doi.org/10.1038/nrd4433.
[5] Wang R, Szabo C, Ichinose F, Ahmed A, Whiteman M, Papapetropoulos A. The role of H_2S bioavailability in endothelial dysfunction. Trends Pharmacol Sci 2015;36:568–78. https://doi.org/10.1016/j.tips.2015.05.007.
[6] Wang R. The Gasotransmitter role of hydrogen sulfide. Antioxidants Redox Signal 2003;5:493–501. https://doi.org/10.1089/152308603768295249.
[7] Zhang H, Xia X, Zhao H, Zhang GN, Jiang DY, Xue XY, Zhang J. A near-infrared fluorescent probe based on SNAr reaction for H_2S/GSH detection in living cells and zebrafish. Dyes Pigments 2019;163:183–9. https://doi.org/10.1016/j.dyepig.2018.11.050.
[8] Sunzini F, De Stefano S, Chimenti MS, Melino S. Hydrogen sulfide as potential regulatory gasotransmitter in arthritic diseases. Int J Mol Sci 2020;21(17):6134. https://doi.org/10.3390/ijms21041180.
[9] Nagahara N, Koike S, Nirasawa T, Kimura H, Ogasawara Y. Alternative pathway of H_2S and polysulfides production from sulfurated catalytic-cysteine of reaction intermediates of 3-mercaptopyruvate sulfurtransferase. Biochem Biophys Res Commun 2018;496:648–53. https://doi.org/10.1016/j.bbrc.2018.01.056.
[10] Pol A, Renkema GH, Tangerman A, Winkel EG, Engelke UF, de Brouwer APM, Lloyd KC, Araiza RS, van den Heuvel L, Omran H, et al. Mutations in SELENBP1, encoding a novel human methanethiol oxidase, cause extraoral halitosis. Nat Genet 2018;50:120–9. https://doi.org/10.1038/s41588-017-0006-7.
[11] Bhattacharyya S, Saha S, Giri K, Lanza IR, Nair KS, Jennings NB, Rodriguez-Aguayo C, Lopez-Berestein G, Basal E, Weaver AL, Visscher DW, Cliby W, Sood AK, Bhattacharya R, Mukherjee P. Cystathionine beta-synthase (CBS) contributes to advanced ovarian cancer progression and drug resistance. PloS One 2013;8(11):e79167. https://doi.org/10.1371/journal.pone.0079167.
[12] Módis K, Bos EM, Calzia E, van Goor H, Coletta C, Papapetropoulos A, Hellmich MR, Radermacher P, Bouillaud F, Szabo C. Regulation of mitochondrial bioenergetic function by hydrogen sulfide. Part II. Pathophysiological and therapeutic aspects. Br J Pharmacol 2014;171:2123–46. https://doi.org/10.1111/bph.12368.
[13] Chen H, Gong X, Liu X, Li Z, Zhang J, Yang XF. A nitroso-based fluorogenic probe for rapid detection of hydrogen sulfide in living cells. Sensor Actuator B Chem 2019;281:542–8. https://doi.org/10.1016/j.snb.2018.10.086.
[14] Zhang H, Xie Y, Wang P, Chen G, Liu R, Lam YW, Hu Y, Zhu Q, Sun H. An iminocoumarin benzothiazole-based fluorescent probe for imaging hydrogen sulfide in living cells. Talanta 2015;135:149–54. https://doi.org/10.1016/j.talanta.2014.12.044.
[15] Liu M, Li Y, Liang B, Li Z, Jiang Z, Chu C, Yang J. Hydrogen sulfide attenuates myocardial fibrosis in diabetic rats through the JAK/STAT signaling pathway. Int J Mol Med 2018;41(4):1867–76. https://doi.org/10.3892/ijmm.2018.3419.
[16] Fiorucci S, Antonelli E, Mencarelli A, Orlandi S, Renga B, Rizzo G, Distrutti E, Shah V, Morelli A. The third gas: H2S regulates perfusion pressure in both the isolated and perfused normal rat liver and in cirrhosis. Hepatology 2005;42(3):539–48. https://doi.org/10.1002/hep.20817.
[17] Pupo E, Pla AF, Avanzato D, Moccia F, Cruz JE, Tanzi F, Merlino A, Mancardi D, Munaron L. Hydrogen sulfide promotes calcium signals and migration in tumor-derivedendothelial cells. Free Radic Biol Med 2011;51:1765–73. https://doi.org/10.1016/j.freeradbiomed.2011.08.007.
[18] Huang Y, Zhang C, Xi Z, Yi L. Synthesis and characterizations of a highly sensitive and selective fluorescent probe for hydrogen sulfide. Tetrahedron Lett 2016;57:1187–91. https://doi.org/10.1016/j.tetlet.2016.02.017.
[19] Kamoun P, Belardinelli MC, Chabli A, Lallouchi K, Chadefaux-Vekemans B. Endogenous hydrogen sulfide overproduction in Down syndrome. Am J Med Genet 2003;116A:310–1. https://doi.org/10.1002/ajmg.a.10847.

[20] Bazhanov N, Escaffre O, Freiberg AN, Garofalo RP, Casola A. Broad-range antiviral activity of hydrogen sulfide against highly pathogenic RNA viruses. Sci Rep 2017; 7:41029. https://doi.org/10.1038/srep41029.

[21] Evgen'ev MB, Frenkel A. Possible application of H_2S-producing compounds in therapy of coronavirus (COVID-19) infection and pneumonia. Cell Stress Chaperones 2020;14:1–3. https://doi.org/10.1007/s12192-020-01120-1.

[22] Zhao Y, Biggs TD, Xian M. Hydrogen sulfide (H_2S) releasing agents: chemistry and biological applications. Chem Commun 2014;50:11788–805. https://doi.org/10.1039/c4cc00968a.

[23] Ismail I, Chen Z, Sun L, Ji X, Ye H, Kang X, Huang H, Song H, Bolton SG, Xi Z, Pluth MD, Yi L. Highly efficient H_2S scavengers via thiolysis of positively-charged NBD amines. Chem Sci 2020;11:7823–8. https://doi.org/10.1039/d0sc01518k.

[24] Yang CT, Wang YY, Marutani E, Ida T, Ni X, Xu S, Chen W, Zhang H, Akaike T, Ichinose F, Xian M. Data-driven identification of hydrogen sulfide scavengers. Angew Chem Int Ed 2019;58:10898–902. https://doi.org/10.1002/anie.201905580.

[25] Szabo C, Coletta C, Chao C, Módis K, Szczesny B, Papapetropoulos A, Hellmich MR. Tumor-derived hydrogen sulfide, produced by cystathionine-β-synthase, stimulates bioenergetics, cell proliferation, and angiogenesis in colon cancer. Proc Natl Acad Sci Unit States Am 2013;110:12474–9. https://doi.org/10.1073/pnas.1306241110.

[26] Giuffrè A, Tomé CS, Fernandes DGF, Zuhra K, Vicente JB. Hydrogen sulfide metabolism and signaling in the tumor microenvironment. Adv Exp Med Biol 2020; 1219:335–53. https://doi.org/10.1007/978-3-030-34025-4_17.

[27] Wu D, Si W, Wang M, Lv S, Ji A, Li Y. Hydrogen sulfide in cancer: friend or foe? Nitric Oxide 2015;50:38–45. https://doi.org/10.1016/j.niox.2015.08.004.

[28] Li H, Xu F, Gao G, Gao X, Wu B, Zheng C, Wang P, Li Z, Hua H, Li D. Hydrogen sulfide and its donors: novel antitumor and antimetastatic therapies for triple-negative breast cancer. Redox Biology 2020;34:101564. https://doi.org/10.1016/j.redox.2020.101564.

[29] Carballal S, Trujillo M, Cuevasanta E, Bartesaghi S, Möller MN, Folkes LK, García-Bereguiaín MA, Gutiérrez-Merino C, Wardman P, Denicola A, Radi R, Alvarez B. Reactivity of hydrogen sulfide with peroxynitrite and other oxidants of biological interest. Free Radic Biol Med 2011;50:196–205. https://doi.org/10.1016/j.freeradbiomed.2010.10.705.

[30] Ubuka T. Assay methods and biological roles of labile sulfur in animal tissues. J Chromatogr B Anal Technol Biomed Life Sci 2002;781:227–49. https://doi.org/10.1016/S1570-0232(02)00623-2.

[31] Doeller JE, Isbell TS, Benavides G, Koenitzer J, Patel H, Patel RP, Lancaster Jr JR. Polarographic measurement of hydrogen sulfide production and consumption by mammalian tissues. Anal Biochem 2005;341:40–51. https://doi.org/10.1016/j.ab.2005.03.024.

[32] Zhao Q, Huo F, Kang J, Zhang Y, Yin C. A novel FRET-based fluorescent probe for the selective detection of hydrogen sulfide (H_2S) and its application for bioimaging. J Mater Chem B 2018;6:4903–8. https://doi.org/10.1039/C8TB01070F.

[33] Dou Y, Gu X, Ying S, Zhu S, Yu S, Shen W, Zhu Q. A novel lysosome-targeted fluorogenic probe based on 5-triazole-quinoline for the rapid detection of hydrogen sulfide in living cells. Org Biomol Chem 2018;16:712–6. https://doi.org/10.1039/C7OB02881D.

[34] Zhang L, Li S, Hong M, Xu Y, Wang S, Liu Y, Qian Y, Zhao J. A colorimetric and ratiometric fluorescent probe for the imaging of endogenous hydrogen sulphide in living cells and sulphide determination in mouse hippocampus. Org Biomol Chem 2014;12:5115–25. https://doi.org/10.1039/C4OB00285G.

[35] Deng B, Ren M, Wang JY, Zhou K, Lin W. A mitochondrial-targeted two-photon fluorescent probe for imaging hydrogen sulfide in the living cells and mouse liver tissues. Sensor Actuator B Chem 2017;248:50–6. https://doi.org/10.1016/j.snb.2017.03.135.

[36] Hu Y, Kang J, Zhou P, Han X, Sun Y, Liu S, Zhang L, Fang J. A selective colorimetric and red-emitting fluorometric probe for sequential detection of Cu^{2+} and H_2S. Sensor Actuator B Chem 2018;255:3155–62. https://doi.org/10.1016/j.snb.2017.09.140.

[37] Hou F, Huang L, Xi P, Cheng J, Zhao X, Xie G, Shi Y, Cheng F, Yao X, Bai D, Zeng Z. A retrievable and highly selective fluorescent probe for monitoring sulfide and imaging in living cells. Inorg Chem 2012;51(4):2454–60. https://doi.org/10.1021/ic2024082.

[38] Ding S, Feng G. Smart probe for rapid and simultaneous detection and discrimination of hydrogen sulfide, cysteine/homocysteine, and glutathione. Sensor Actuator B Chem 2016;235:691–7. https://doi.org/10.1016/j.snb.2016.05.146.

[39] Zhang L, Zheng XE, Zou F, Shang Y, Meng W, Lai E, Xu Z, Liu Y, Zhao J. A highly selective and sensitive near-infrared fluorescent probe for imaging of hydrogen sulphide in living cells and mice. Sci Rep 2016;6:18868. https://doi.org/10.1038/srep18868.

[40] Zhang X, Jin X, Zhang C, Zhong H, Zhu H. A fluorescence turn-on probe for hydrogen sulfide and biothiols based on PET & TICT and its imaging in HeLa cells. Spectrochim Acta A Mol Biomol Spectrosc 2021;244:118839. https://doi.org/10.1016/j.saa.2020.118839.

[41] Ma B, Tian D, Yan S, Li X, Dai F, Zhou B. Developing a styrylpyridinium-based fluorescent probe with excellent sensitivity for visualizing basal H_2S levels in mitochondria. Sensor Actuator B Chem 2021;327:1289372. https://doi.org/10.1016/j.snb.2020.128937.

[42] Lv J, Wang F, Qiang J, Ren X, Chen Y, Zhang Z, Wang Y, Zhang W, Chen X. Enhanced response speed and selectivity of fluorescein-based H_2S probe via the cleavage of nitrobenzene sulfonyl ester assisted by ortho aldehyde groups. Biosens Bioelectron 2017;87:96–100. https://doi.org/10.1016/j.bios.2016.08.018.

[43] Jin X, Wu S, She M, Jia Y, Hao L, Yin B, Wang L, Obst M, Shen Y, Zhang Y, Li J. Novel fluorescein-based fluorescent probe for detecting H_2S and its real applications in blood plasma and biological imaging. Anal Chem 2016;88(22): 11253–60. https://doi.org/10.1021/acs.analchem.6b04087.

[44] Forkner MW, Rieke RD. The synthesis of new electron-deficient naphthoquinones. Synth Met 1996;79:197–200. https://doi.org/10.1016/0379-6779(96)80192-5.

[45] Turovska B, Stradins J, Freimanis J, Strazdins I, Logins J, Dregeris J. Electrochemical study of intramolecular charge transfer complexes derived from 1,4-naphthoquinone. Part 2. Electro-oxidation of 2-substituted 3-arylamino-l,4-naphthoquinone autocomplexes. J Electroanal Chem 1996;414:221–7. https://doi.org/10.1016/0022-0728(96)04683-9.

[46] Li H, Cai L, Chen Z, Wang W. Advances in chemical sensors: coumarin-derived fluorescent chemosensors. Intech 2012:121–51. https://doi.org/10.5772/33157.

[47] Tandon VK, Maurya HK. Facile and efficient synthesis of novel oxazine, oxazepine and phenoxazine of chromenones fused with 1,4-naphthoquinone. Heterocycles 2009;77:611–5. https://doi.org/10.3987/COM-08-S(F)30.

[48] Yamaji M, Kurumi M, Kimura H, Shizuka H. Hydration effects on the triplet exciplex between 2,3-dihalo-1,4-naphthoquinone and furan studied by steady-state and laser flash photolysis. Phys Chem Chem Phys 1999;1:1859–65. https://doi.org/10.1039/A809483G.

[49] Sun W-C, Gee KR, Haugland RP. Synthesis of novel fluorinated coumarins: excellent UV-light excitable fluorescent dyes. Bioorg Med Chem Lett 1998;8: 3107–10. https://doi.org/10.1016/S0960-894X(98)00578-2.

[50] Wang L, Li Y, Li G, Xie Z, Ye B. Electrochemical characters of hymecromone at the graphene modified electrode and its analytical application. Anal Methods 2015;7: 3000–5. https://doi.org/10.1039/c4ay03051f.

[51] Pallu J, Rabin C, Creste G, Branca M, Mavré F, Limoges B. Exponential molecular amplification by H_2O_2 mediated autocatalytic deprotection of boronic ester probes to redox cyclers. Chem Eur J 2019;25:7534–46. https://doi.org/10.1002/chem.201900627.

[52] Glowacka PC, Maindron N, Stephenson GR, Romieu A, Renard P-Y, daSilva Emery F. Synthesis and photophysical properties of iron-carbonyl complex-coumarin conjugates as potential bimodal IR-fluorescent probes. Tetrahedron Lett 2016;57:4991–6. https://doi.org/10.1016/j.tetlet.2016.09.091.

[53] Taniguchi M, Lindsey JS. Database of absorption and fluorescence spectra of >300 common compounds for use in PhotochemCAD. Photochem Photobiol 2018;94: 290–327. https://doi.org/10.1111/php.12860.

[54] Wang R, Li Z, Zhang C, Li Y, Gu X, Zhang H, Yi L, Xi Z. Fast response turn-on fluorescent probes based on thiolysis of NBD amine for H_2S bioimaging. Chembiochem 2017;163:962–8. https://doi.org/10.1002/cbic.201600060.

[55] Zhang J, Wang R, Zhu Z, Yi L, Xi Z. A FRET-based ratiometric fluorescent probe for visualizing H_2S in lysosomes. Tetrahedron 2015;71:8572–6. https://doi.org/10.1016/j.tet.2015.09.028.

[56] Kaflea A, Bhattaraia S, Miller J, Scott T, Handy S. Hydrogen sulfide sensing using an aurone-based fluorescent probe. RSC Adv 2020;10:45180–8. https://doi.org/10.1039/D0RA08802A.

[57] Schendorf T, Vecchio R, Koech K, Blough N. A standard protocol for $NaBH_4$ reduction of CDOM and HS. Limnol Oceanogr: Methods 2016;14:414–23. https://doi.org/10.1002/lom3.10100.

[58] Zhang Y, Wang J, Yue Y, Chao J, Huo F, Yin C. A new strategy for the fluorescence discrimination of Cys/Hcy and GSH/H_2S simultaneously colorimetric detection for H_2S. Spectrochim Acta A Mol Biomol Spectrosc 2020;227:117537. https://doi.org/10.1016/j.saa.2019.117537.

[59] Ou L, Lin W. A coumarin-based "off–on" fluorescent probe for highly selective detection of hydrogen sulfide and imaging in living cells. Anal. Methods 2021;13: 1511–6. https://doi.org/10.1039/D1AY00097G.